Biosystems Engineering (2005) 91 (4), 403–411
doi:10.1016/j.biosystemseng.2005.05.003
AE—Automation and Emerging Technologies

Neural Network for estimating Vehicle Behaviour on Sloping Terrain

Z.X. Zhu[1]; R. Torisu[1]; J.I. Takeda[1]; E.R. Mao[2]; Q. Zhang[3]

[1]Faculty of Agriculture, Iwate University, Morioka 020-8550, Japan; e-mail of corresponding author: u0203008@iwate-u.ac.jp
[2]College of Engineering, China Agricultural University, Beijing 100083, China; e-mail: gxy15@cau.edu.cn
[3]Department of Agricultural Engineering, University of Illinois, Illinois 61801, USA; e-mail: qinzhang@uiuc.edu

(Received 3 September 2004; accepted in revised form 6 May 2005; published online 29 June 2005)

This paper presents formulation of a neural network (NN) vehicle model for estimating vehicle behaviour on sloping terrain. Lemniscate of Bernoulli courses were employed to acquire training pairs. A training method combined with genetic algorithm and back propagation algorithm was used to train the NN vehicle model. The model was validated by comparing the simulated results with the experimental ones. The open-loop characteristics of vehicle motion on sloping terrain were also investigated. A fuzzy logic controller based on the constructed NN vehicle model guided the tractor along a pre-determined path successfully with mean and standard lateral deviation of 0·005 m and 0·067 m, respectively. The results indicated that the NN vehicle model was qualified to represent the input–output relationship of the vehicle motion for autonomous navigation on sloping terrain.

1. Introduction

Most farm mobile robot systems are non-linear time invariant, and are subject to non-holonomic systems. Therefore, an effective approach must be taken to measure the system performance. Generally, vehicle models are used for this purpose. A kinematic model is usually applicable for slow speed vehicles where effects of side forces can be neglected (Ishida *et al.*, 1998; Cordesses *et al.*, 2000; Roth & Batavia, 2002). However, a dynamic model takes into account the lateral forces at wheels, the mass of the vehicle, the mass moment of inertia of the vehicle, and the location of the centre of gravity. Consequently, the dynamic model is widely applied in farm vehicle automatic navigation systems (Miller & Steward, 2002; Kise *et al.*, 2002). In addition, an artificial intelligence (AI) model was also developed by Ishii *et al.* (1998). However, these models were developed mostly to describe vehicle behaviour on flat land where friction properties were relatively constant.

On sloping ground, many factors influence vehicle behaviour such as terrain slope, lateral slippage, and so on. Therefore, it is necessary to develop a more suitable model for vehicle motion on sloping terrain. In order to control a tractor along a course on sloping terrain, Bell (2000) introduced a form of bias estimation into the control software to enable more accurate control. However, the highly simplified dynamic model he used did not incorporate the terrain slope. Torisu *et al.* (2002) designed a neural network (NN) vehicle model instead of a dynamic or kinematic model to express the input-output relationship of vehicle motion on sloping land. However, the model could represent only the motion on a specific slope and the heading angle was restricted within $-60°$ to $60°$. A new vehicle kinematic model accounting for sliding effects was developed by Lenain *et al.* (2003). According to this model, an adaptive control scheme was proposed to navigate a car-like mobile robot along a straight path on sloping ground. However, if the robot followed a curvous path on sloping ground, the sliding parameters quickly changed. In this condition, as mentioned by the authors, the lateral deviation would increase.

This paper presents construction of an NN vehicle model that can express the dynamic characteristics of the vehicle. A fuzzy logic controller based on the constructed NN vehicle model is used to guide the tractor along a pre-determined path on sloping terrain. To attain this task our research sets out to (1) construct an NN vehicle

Notation

A	amplitude, m	W_{ij}^{pq}	weight between two neurons
a	constant	x, y	co-ordinates of the courses, m
C	defined maximum error	x_{Gk}, y_{Gk}	co-ordinates of vehicle centre of gravity, m
E	mean square error of an individual	Δx_{Gk}, Δy_{Gk}	velocities of vehicle centre of gravity along X and Y axes in the earth fixed frame, m/s
f	fitness of an individual	$\boldsymbol{z}_k$	state vector
i	row number of neurons	α_k	steering angle, deg
j	row number of neurons	$\Delta\alpha_k$	rate of steering, deg/s
l	wavelength, m	β_k	sideslip angle, deg
N	net input of a neuron	θ_k	heading angle, deg
p	layer number	λ	value of input or output
p_Q	input to the network	λ_{max}	maximum of the corresponding input or output variable
q	layer number	ξ_{k+1}	output vector
t_Q	corresponding target output	φ_k	terrain slope, deg
Δt	sampling time, s	ω_k	yaw rate, deg/s
$\boldsymbol{u}_k$	control vector		
V_k	vehicle velocity in the earth fixed frame, m/s	*Subscripts*	
V_{xk}	forward velocity of vehicle centre of gravity in the vehicle fixed frame, m/s	k	time step
V_{yk}	lateral velocity of vehicle centre of gravity in the vehicle fixed frame, m/s		

model, (2) train the NN vehicle model with the genetic algorithm (GA) and back propagation (BP), (3) validate the model, (4) investigate the open-loop characteristics of vehicle motion on sloping terrain, and (5) conduct a path-tracking test on sloping terrain.

2. Construction of neural network vehicle model for sloping terrain

2.1. *Structure of the neural network vehicle model*

The principles for formulating NN vehicle model, as in all modelling problems, seek to use the simplest network that can adequately represent the training set (or training pairs). For a network to be able to successfully generalise what it has learned to other data set, it should have fewer parameters than there are samples in the training set (Hagan *et al.*, 1996).

The architecture of the constructed NN model was 7-6-5-3, as shown in *Fig. 1*. The input layer, the first hidden layer, the second hidden layer, and the output layer had seven, six, five, and three neurons, respectively. The input vector is a combination of the control vector $\boldsymbol{u}_k$ and the state vector $\boldsymbol{z}_k$, and the output vector is $\boldsymbol{\xi}_{k+1}$:

$$\boldsymbol{u}_k = (\alpha_k, \Delta\alpha_k)^{\mathrm{T}} \tag{1}$$

$$\boldsymbol{z}_k = (V_{xk}, V_{yk}, \omega_k, \theta_k, \varphi_k)^{\mathrm{T}} \tag{2}$$

$$\boldsymbol{\xi}_{k+1} = (V_{xk+1}, V_{yk+1}, \omega_{k+1})^{\mathrm{T}} \tag{3}$$

where: α_k is the steering angle in deg; $\Delta\alpha_k$ is the rate of steering in deg/s; V_{xk} is the forward velocity of vehicle centre of gravity in the vehicle fixed frame in m/s; V_{yk} is the lateral velocity of vehicle centre of gravity in the vehicle fixed frame in m/s; θ_k is the heading angle in deg; ω_k is the yaw rate of the vehicle in deg/s; φ_k is the terrain slope in deg; and the subscript k means equally spaced time step ($k = 1, 2, 3, \ldots$) in a discrete system. The output vector ξ_{k+1} represents the vehicle state after each 0·5 s. The output is determined by both the current inputs and their previous outputs. The sigmoid transfer function of the model, as shown in Eqn (4), was used as the threshold function,

$$f(N) = \frac{1}{1 + \mathrm{e}^{-N}} \tag{4}$$

where N is the net input of a neuron.

Compared with the NN vehicle model formulated by Torisu *et al.* (2002), the constructed one was incorporated with incline information φ_k, so that it could be applicable for different gradients and not just for a particular gradient. Although the inputs increased, the adjustable weights and biases decreased from 105 to 101. This lowered the probability of trapping in a local optimum when the model was trained.

2.2. *Experimental equipment and experimental conditions*

An 18 kW four-wheel drive Mitsubishi MT2501D model tractor was modified to serve as the test tractor.

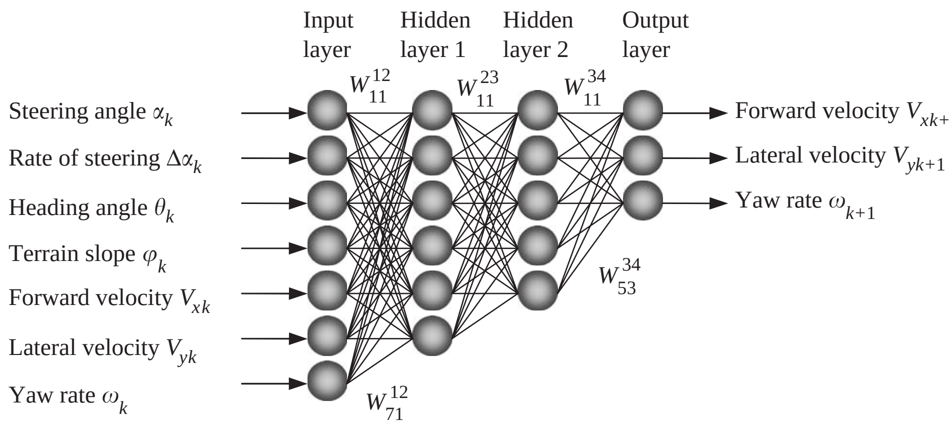

Fig. 1. Architecture of the neural network (NN) vehicle model: α_k, steering angle; $\Delta\alpha_k$, rate of steering; V_{xk}, forward velocity; V_{yk}, lateral velocity; θ_k, heading angle; ω_k, yaw rate; φ_k, terrain slope; k, time step; W_{ij}^{pq}, weight; p and q, consecutive layer number; i and j, row numbers

Total mass of the tractor was 1125 kg with a wheelbase of 1·595 m and tread of 1·310 m. The tyres were high lug type with an inflation pressure of 0·2 MPa for front tyre and 0·1 MPa for rear tyre. *Figure 2* shows the prototype test tractor with sensors and equipment. The specifications of instrumentation used in the experiments are listed in Table 1.

All tests were conducted in November 2003 on a sloping meadow at Iwate University Omyojin Research Farm in Japan. The surface of the meadow was undulating and covered with grass. The soil condition was moderately moist and soft in some places. Due to the limitation of the test field, the data acquisition test was performed only in one place, where the average land inclination, standard deviation, and variance of the test course were 9·96°, 1·57°, and 2·46°, respectively.

Fig. 2. Prototype test tractor with sensors and equipment

2.3. *Data acquisition*

A skilled human operator operated the test tractor along the pre-determined lemniscate of Bernoulli courses (*Fig. 3*) in an initially clockwise direction and in an initially anticlockwise direction, course 1 and course 2, respectively. The courses were described by

$$(x^2 + y^2)^2 = 2a^2(x^2 - y^2) \tag{5}$$

where: x and y are the co-ordinates of the courses and a is a constant with a value in this case of 6·0 The centreline (X axis) is parallel to the contour line and the Y axis is towards the uphill direction.

The vehicle forward velocity was set at 0·5 m s^{-1}. Since the sampling time interval of the vehicle positioning sensor (Total station) was inconsistent, vehicle locations were measured by an alternative way after a regular interval 0·5 s. The locations were marked on the ground by spraying coloured ink from a pressurised intravenous drip container mounted on the tractor. The tractor mounted computer controlled the timing of ink spraying. Recordings of vehicle heading angle, steering angle, vehicle speed, and terrain slope were also synchronised with the ink spraying. Vehicle positions were measured using a laser positioning system. Locations of vehicle centre of gravity were calculated from the positions of ink spray and heading angle. Referring to *Fig. 4*, the other variables of input/output pairs were also calculated from the recorded data by:

$$\Delta\alpha_k = \frac{\alpha_{k+1} - \alpha_k}{\Delta t} \tag{6}$$

$$\Delta x_{Gk} = \frac{x_{Gk+1} - x_{Gk}}{\Delta t} \tag{7}$$

$$\Delta y_{Gk} = \frac{y_{Gk+1} - y_{Gk}}{\Delta t} \tag{8}$$

Table 1
Specification of instrumentation

Equipment	*Function*
DC motor	Power is 82 W, used for the steering actuator
1·0 GHz Pentium PC	Mounted on the tractor, used as the central processing unit
Potentiometer	Fixed on the front axle, measured the steering angle
Magnetic sensor	Fixed near the flywheel, measured the engine speed
Fibre optic gyroscope (FOG)	Model is JG-35FD, used to measure the heading angle with range of $\pm 180°$, angular drift is less than $\pm 1{\cdot}5°\ h^{-1}$
Total station (TS) and prism	Leica TCA 1105 model, 2 mm positioning accuracy
Wireless modems	Transmit the signals of the tractor position from the TS to the PC
AD/DA board	Converts the analogue signals to digital (AD) and digital to analogue (DA)
Sprayer	Marks the vehicle locations by spraying colour ink
Inclinometer	TCM-2X-90 model, measured the pitch and roll

DC, direct current; PC, personal computer.

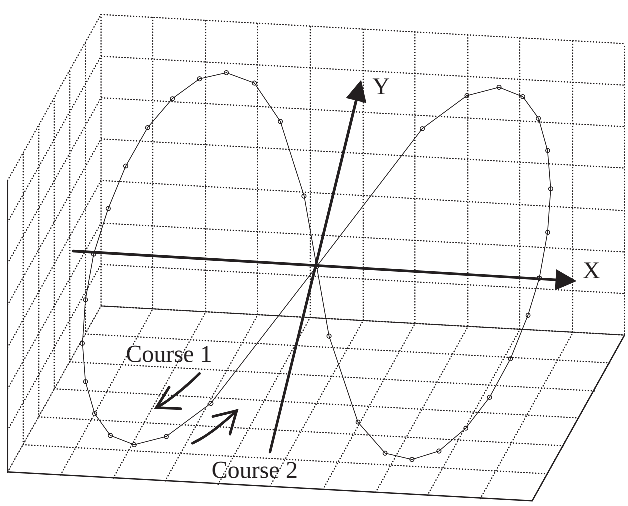

Fig. 3. Lemniscate of Bernoulli courses: X, *in the contour line direction;* Y, *in an uphill direction; course 1, in an initially clockwise direction; course 2, in an initially anticlockwise direction*

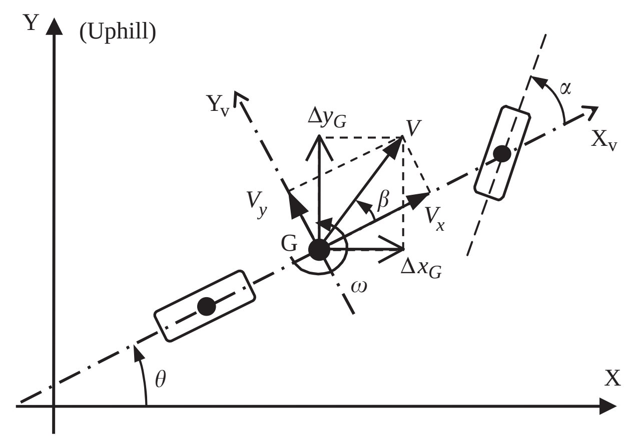

Fig. 4. Vehicle dynamic motions on sloping terrain: X, *in the contour line direction;* Y, *in an uphill direction;* X_v *and* Y_v, *axes of the vehicle fixed frame; G, vehicle center of gravity; V, vehicle velocity in the earth fixed frame;* V_x *and* V_y, *forward and lateral velocities of vehicle center of gravity in the vehicle fixed frame, respectively;* Δx_G *and* Δy_G, *velocities along* X *and* Y *axes in the earth fixed frame, respectively;* α, *steering angle;* β, *sideslip angle;* θ, *heading angle;* ω, *yaw rate*

$$\beta_k = \tan^{-1}\left(\frac{\Delta y_{Gk}}{\Delta x_{Gk}}\right) - \theta_k \tag{9}$$

$$V_k = \frac{\Delta x_{Gk}}{\cos(\theta_k + \beta_k)} \tag{10}$$

$$\omega_k = \frac{\theta_{k+1} - \theta_k}{\Delta t} \tag{11}$$

$$V_{xk} = V_k \cos \beta_k \tag{12}$$

$$V_{yk} = V_k \sin \beta_k \tag{13}$$

where: Δt is sampling time in s; x_{Gk} and y_{Gk} are the co-ordinates of vehicle centre of gravity in m; Δx_{Gk} and Δy_{Gk} are the velocities of vehicle centre of gravity along X and Y axes in the earth fixed frame, respectively, in m/s; β_k is the sideslip angle in deg; V_k is the vehicle velocity in the earth fixed frame in m/s; and the subscript k is sampling time step ($k = 1, 2, 3, \ldots$).

Before training, all the input/output variables were normalised to range from 0 to 1. The forward velocity of vehicle centre of gravity V_{xk} and the terrain slope φ_k were normalised by Eqn (14), and the others were normalised by Eqn (15):

$$f(\lambda) = \frac{\lambda}{\lambda_{max}} \tag{14}$$

$$f(\lambda) = \frac{\lambda + \lambda_{max}}{2\lambda_{max}} \tag{15}$$

where: λ is a value of input or output and λ_{max} is the maximum of the corresponding input or output variable.

The data set acquired with the lemniscate of Bernoulli courses was representative of a much larger class of possible input/output pairs. There were 346 pairs in the data set acquired with course 1 and course 2. The steering angle ranged from $-34{\cdot}6°$ to $37{\cdot}2°$; the terrain slope ranged from $6{\cdot}0°$ to $14{\cdot}9°$; the heading angle ranged from $-180°$ to $180°$. The data set (346 samples) was randomly separated into a training set (306 samples) and a test set (40 samples).

2.4. *Training of the neural network model*

A supervised training method, called a BP algorithm, together with a GA was used to train the NN model. The learning rule of BP is provided with a set of examples (the training set) of proper network behaviour: $\{p_1, t_1\}, \{p_2, t_2\}, \ldots, \{p_Q, t_Q\}$, where p_Q is an input to the network and t_Q is the corresponding target output. As the inputs are applied to the network, the network outputs are compared to the targets. The learning rule is then used to adjust the weights and biases of the network in order to move the network outputs closer to the targets.

Although the BP algorithm has a strong ability for local searching, it easily traps in a local optimum if the multilayer network has many local minima (Hagan *et al.*, 1996). For this problem, GA offers a preferable solution with the attraction that all parts of the feasible space are potentially available for exploration, so the global minimum should be attained if premature convergence can be avoided (Chambers, 1995). On the other hand, the GA is often slow for local optimisation. Therefore, a combination of GA and BP algorithms was applied to train the NN model.

Figure 5 shows the flowchart of the training procedure. The GA procedure was composed of the steps in the dashed rectangle. The chromosome of the GA was composed of the weights in the NN vehicle model with a length of 101, the format of which is described as follows:

$$W^{12}_{11}, W^{12}_{12}, \ldots, W^{12}_{86}, W^{23}_{11}, \ldots, W^{23}_{75}, W^{34}_{11}, \ldots, W^{34}_{63}$$

The GA was executed 200 times. The GA parameters in this case are described as follows: the population size was 60; mutation rate varied from 0·05 to 0·15; two-point crossover with a crossover rate of 0.6; roulette wheel selection. The fitness of each individual in the GA was calculated by

$$f = \begin{cases} C - E, & E < C \\ 0, & E \geqslant C \end{cases} \tag{16}$$

where: f is the fitness of an individual; E is the mean square error of the same individual; and C is the defined maximum error with a value of 0·5.

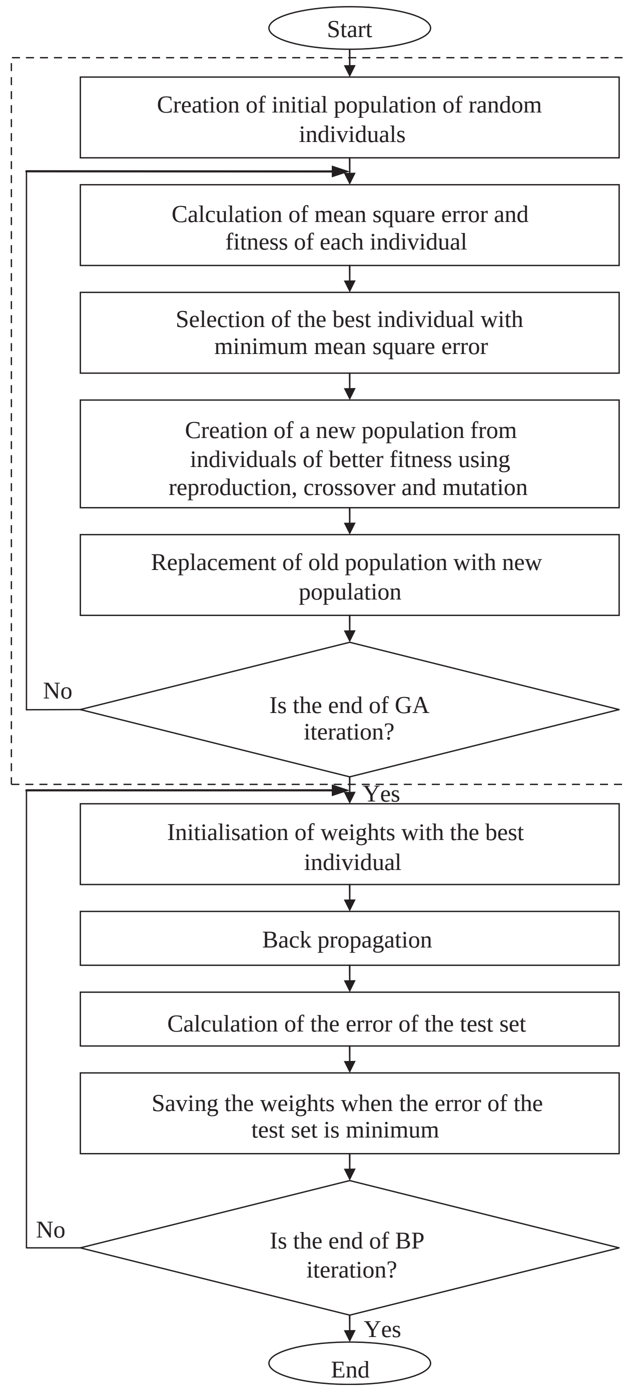

Fig. 5. Flowchart of training the neural network (NN) vehicle model: GA, genetic algorithm; BP, back propagation

In order to prevent premature convergence and keep the population diversity, some measures were taken. During selection, some individuals whose fitness was better than the average fitness were discarded and replaced with random values. The mutation rate increased with the iteration number.

After finishing the GA processing, the BP began to be executed. The weights of the NN vehicle model were initialised with the best individual derived from the GA processing. The iteration times of BP were 220 000. During training, the weights were saved when the mean square error of the test set was minimum.

2.5. *Model validation*

2.5.1. *Validation by the lemniscate of Bernoulli courses*

To validate the NN model, simulations for course 1 and course 2 were conducted and the simulation results were compared to experimental ones. In the simulation, since steering angle was the only control input, the derivative $\Delta\alpha$ of the same steering angle recorded during the data acquisition test was used as the control input. In the beginning, input variables of the NN model were initialised to the first recorded data in the test. After that, the terrain slope and rate of steering were input to the NN model with their actual values acquired in test, whereas the rest of the variables were calculated. For every step of calculation, the output values were used as the corresponding input values in the next step.

2.5.2. *Generalisation of the neural network vehicle model*

For the purpose of checking the generalisation of the developed NN model, the test with a sinusoidal course was also performed in the same field using a similar procedure as in the data acquisition test. The sinusoidal course was expressed by

$$y = A \sin\left(\frac{2\pi}{l} x\right) \tag{17}$$

where x and y are the co-ordinates of the course; A is the amplitude with a value of 2 m; and l is the wavelength with a value of 16 m. The X axis is parallel to the contour line, and the Y axis is towards the uphill direction.

The simulation was also carried out with the same steps as described in Section 2.4.1.

3. Vehicle behaviour on sloping terrain

3.1. *Characteristics of open-loop control*

The open-loop characteristics of vehicle motion on sloping terrain were investigated by the simulations and experiments. The simulation results were compared to the experimental ones. The comparative cases included rectilinear motion and circular motion on sloping land.

Instead of manual operation, the tractor-mounted personal computer (PC) and other equipment were used to operate the tractor in these tests. For each test, the PC generated the designed steering-actuation signals and accordingly the direct current (DC) motor rotated the steering wheel. The 0° heading angle was always set parallel to the contour line. The tractor velocity was set constant at 0·5 m/s.

Since the sampling time interval of the vehicle positioning sensor used was inconsistent and the constructed NN model was only for 0·5 s interval, the slope angle acquired in the experiment was not the corresponding value in the simulation for every time step. Therefore, during simulations, the slope angle was set to its average in the field test, while the sampling time interval was still set constant at 0·5 s. Other variables were set only at the beginning of simulations, and their values were the same as the first data acquired in the field test.

3.2. *Performance of path tracking*

Every vehicle model is formulated for a certain agricultural application. A fuzzy logic controller was designed to automatically guide the tractor along any rectilinear path on sloping terrain based on the constructed NN vehicle model (Zhu *et al.*, 2004). At the same time, the designed fuzzy controller could also be used for navigating the tractor along curvous paths. The experiment on tracking a pre-determined path composed of a curve and straight lines was conducted on the sloping meadow. Similarly, the 0° heading angle was always set parallel to the contour line and the tractor velocity was set constant at 0·5 m/s.

4. Results and discussion

4.1. *Neural network vehicle model training*

The trajectories of mean squared errors for NN model training are shown in *Fig. 6*. After about 60 000 iterations, the changes of the errors tended to be stable. Although the error of the training set continued to decrease, that of the test set increased. Thus, the weights obtained when the mean square error of the test set was minimum were selected as the final result.

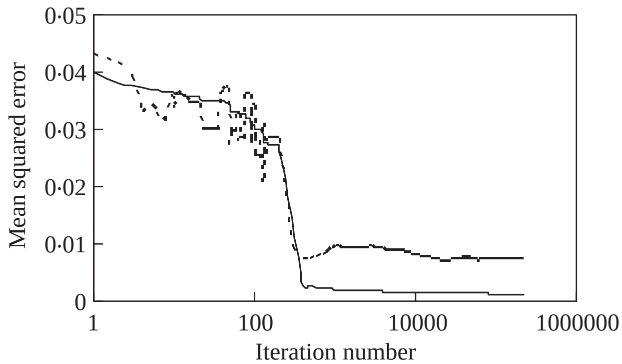

Fig. 6. Trajectories of mean squared error: —, training set; - - -, test set

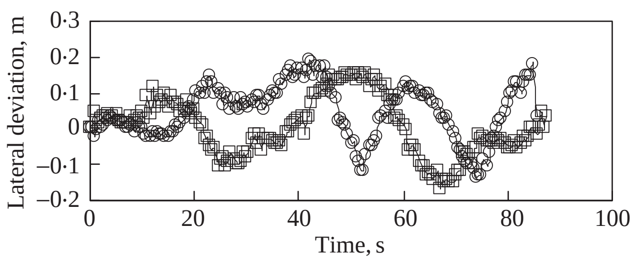

Fig. 7. Time histories of lateral deviation for lemniscate of Bernoulli courses: —□—, in an initially anticlockwise direction; —○—, in an initially clockwise direction

4.2. *Model validation by the lemniscate of Bernoulli courses*

Figure 7 displays the time histories of lateral deviation between the simulated trajectory and the experimental one for the lemniscate of Bernoulli courses, namely course 1 and course 2. For both courses, the mean and standard lateral deviations were 0·026 m and 0·081 m, respectively. The time histories of heading deviation between the simulated trajectory and experimental one are shown in *Fig. 8*. For both courses, the average heading deviation was −0·02° with its standard deviation of 6·54°. The results of the above two figures mean that the actual and simulated trajectories were almost the same. The trained NN model was capable of expressing the vehicle motion on sloping terrain for the lemniscate of Bernoulli courses applied in the data acquisition test.

4.3. *Generalisation of the constructed neural network vehicle model*

Figure 9 shows the time history of lateral deviation between the trajectories of experiment and simulation

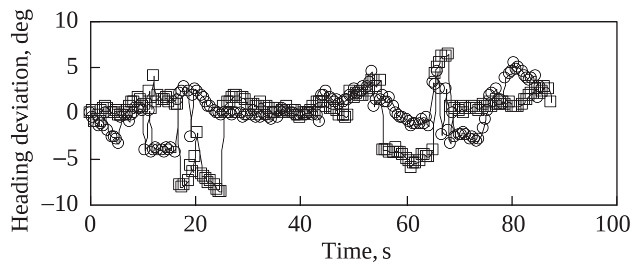

Fig. 8. Time histories of heading deviation for lemniscate of Bernoulli courses: —□—, in an initially anticlockwise direction; —○—, in an initially clockwise direction

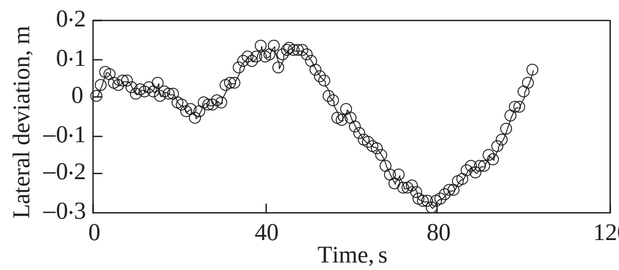

Fig. 9. Time history of lateral deviation for sinusoidal course

for the sinusoidal course. The mean and standard deviation of the lateral deviation were −0·047 and 0·123 m, respectively. Apparently, the NN model could produce outputs near the true responses. Taking account of the variation of soil condition, the accuracy of this test was acceptable. Therefore, it is concluded that the constructed NN vehicle model generalised well.

4.4. *Characteristics of open-loop control*

Figure 10 shows the trajectories of the rectilinear vehicle motion on a 10° slope. Both the experimental and the simulated cases were initialised with same conditions. For the test of travelling along a contour line, the steering angle was fixed at 0° and the heading angle was initialised to 0°. For the test of travelling along an inverted contour line, the steering angle was also fixed at 0°, but the heading angle was initialized to −180°. The time histories of lateral deviation between the experimental and simulated results are shown in *Fig. 11*. For both rectilinear motions, the mean lateral deviation was 0·091 m with its standard deviation of 0·044 m. The results indicate that the simulated results were similar to the actual ones, and that the reconstructed NN model could represent the actual vehicle motion on the sloping land.

Figure 12 shows the trajectories of the anticlockwise circular turn on sloping terrain, where the average

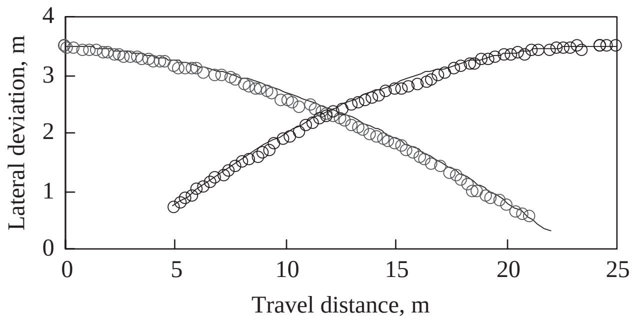

Fig. 10. Trajectories of traveling along contour line and inverted contour line on sloping terrain: ○, actual; —, simulated

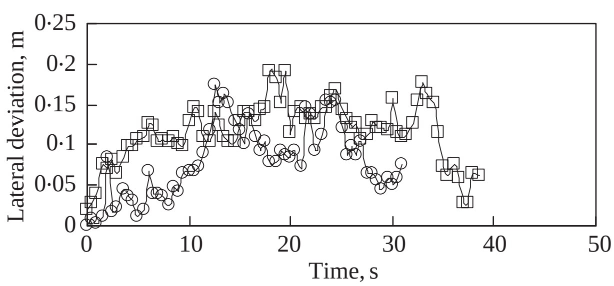

Fig. 11. Time histories of lateral deviation for rectilinear motion with open-loop control: —□—, in the contour line direction; —○—, in the inverted contour line direction

inclination was 10·4°, and varied in the range from 7·2° to 14·5°. The steering angle was fixed at 30° throughout the test. *Figure 13* shows the clockwise circular turn for the same place depicted in *Fig. 12*, but at the bottom of the test field, where the average slope inclination was 9°, and varied in the range from 7·5° to 10·4°. The steering angle was fixed at −30°.

From *Figs 12* and *13*, one important fact became clear: in circular turns, the vehicle deviation on sloping land was not directly downward, which was not so readily thought prior to this test, rather it was along the diagonal between the contour line and downhill direction. For both experiments and simulations, the deviation tendencies were oriented with respect to a contour line of about −42° for the anticlockwise circular turn and about −138° for the clockwise circular turn. The results show that the deviation tendencies resulting from simulation with the NN model are almost similar to those in the tests.

4.5. *Performance of path tracking*

Figure 14 shows the autonomous travelling trajectories along the pre-determined course. The time history of lateral deviation is displayed in *Fig. 15*. The mean and

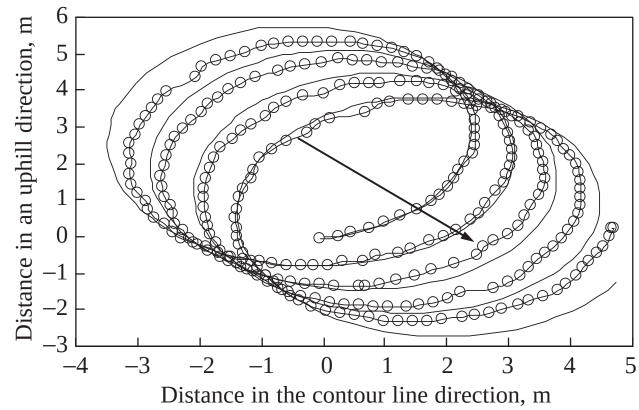

Fig. 12. Trajectories of the anticlockwise circular turn on sloping terrain: —○—, actual; —, simulated

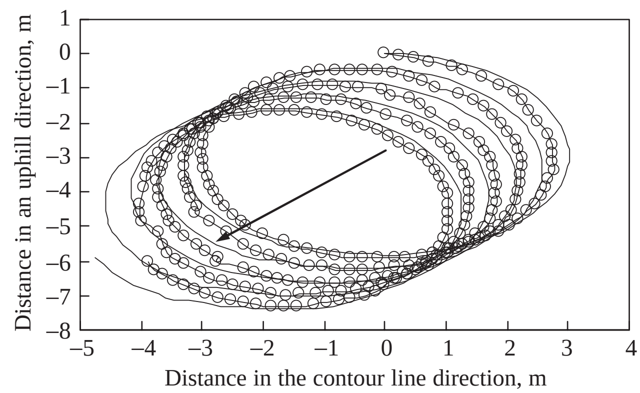

Fig. 13. Trajectories of the clockwise circular turn on sloping terrain: —○—, actual; —, simulated

standard deviation of the tracking errors for the whole course were 0·005 and 0·067 m, respectively, and those for the straight parts were −0·016 and 0·044 m, respectively. Thus, the level of tracking error is acceptable for agricultural operation on grass land.

5. Conclusions

A neural network (NN) vehicle model was formulated and trained by genetic algorithm (GA) and back propagation (BP). Data acquisition tests with lemniscate of Bernoulli courses guaranteed that the NN model was accurate over a wider range. The NN model was validated by the lemniscate of Bernoulli courses and the sinusoidal course. The results showed that the NN model was available and generalised well. From the comparative study of the experiments and simulations of the open-loop characteristics of vehicle motion it was clear that the NN model was qualified to represent the input–output relationship of the vehicle motion on

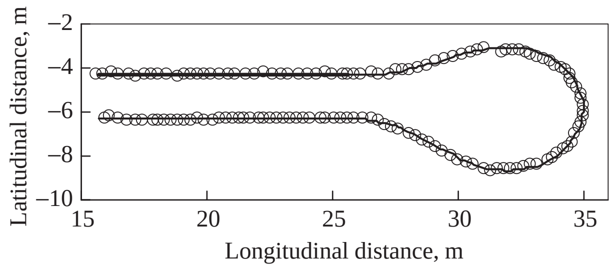

Fig. 14. Automatic travel along a pre-determined path on sloping terrain: ○, actual; —, referenced

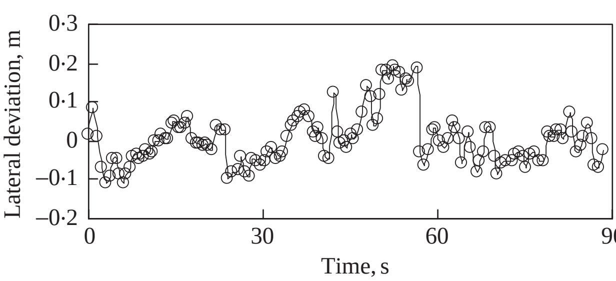

Fig. 15. Time history of lateral deviation for tracking the pre-determined path on sloping terrain

slope-land environment. A fuzzy logic controller based on the constructed NN vehicle model guided the tractor along the pre-determined path successfully with the mean and standard lateral deviation of 0·005 and 0·067 m, respectively. The results indicated further that the NN vehicle model was qualified to represent the vehicle motion for autonomous navigation of the tractor on sloping terrain.

Nevertheless, there is a limitation of the constructed NN vehicle model. The changes of field and soil conditions (e.g. rain) decrease the accuracy of the model. Further work needs to be conducted to improve the accuracy of the model for all field and soil conditions, such as training the NN vehicle model online.

References

Bell T (2000). Automatic tractor guidance using carrier-phase differential GPS. Computers and Electronics in Agriculture, **25,** 53–66

Chambers L (1995). Practical Handbook of Genetic Algorithms: Applications, Vol. I. CCR Press Inc., Boca Raton, FL, USA

Cordesses L; Cariou C; Berducat M (2000). Combine harvester control using real time kinematic GPS. Precision Agriculture, **2,** 147–161

Hagan M T; Demuth H B; Beale M (1996). Neural Network Design. PWS Publishing Company, Boston, MA

Ishida M; Imou K; Okado A; Takenaga H; Honda Y; Itokawa N; Shibuya Y (1998). Autonomous tractor for forage production. Journal of the Japanese Society of Agricultural Machinery, **60**(2), 59–66 (in Japanese)

Ishii K; Terao H; Noguchi N; Kise M (1998). Studies on self learning autonomous vehicles (part 4); online neuro-controller. Journal of the Japanese Society of Agricultural Machinery, **60**(2), 53–57

Kise M; Noguchi N; Ishii K; Terao H (2002). Field mobile robot navigation by RTK-GPS and FOG (part 3). Journal of the Japanese Society of Agricultural Machinery, **64**(2), 102–110 (in Japanese)

Lenain R; Thuilot B; Cariou C; Martinet P (2003). Rejection of sliding effects in car like robot control: application to farm vehicle guidance using a single RTK GPS sensor. Proceedings of the IEEE/RSJ International Conference on Intelligent Robots and Systems,, Vol. 4, 3811–3816

Miller M A; Steward B L (2002). Control and evaluation methods for multi-mode steering. Proceeding of the 26–27 July, 2002 Conference on Automation Technology for Off-Road Equipment, Chicago, Illinois, USA, pp 357–366.

Roth S A; Batavia P H (2002). Evaluating path tracker performance for outdoor mobile robots. Proceeding of the 26–27 July, 2002 Conference on Automation Technology for Off-Road Equipment, Chicago, Illinois, USA, pp 388–397

Torisu R; Hai S; Takeda J; Ashraf M A (2002). Automatic tractor guidance on sloped terrain (part 1); formulation of NN vehicle model and design of control law for contour line travel. Journal of the Japanese Society of Agricultural Machinery, **64**(6), 88–95

Zhu Z X; Torisu R; Takeda J I; Chen J (2004). Autonomous guidance of tractor along arbitrary rectilinear path on sloped terrain. Proceedings of 2004 CIGR International Conference in Beijing, China, Paper No. 50-068A